

Concluding Remarks

Triple-chain ammonium amphiphiles that contain fluorocarbon chains were shown to undergo spontaneous bilayer assemblage in water. The phase-transition behavior and the membrane fluidity are strongly affected by the number of the fluorocarbon tail. The phase-separation behavior is largely determined by the number of the fluorocarbon tail in an amphiphile. The controllable miscibility and the different molecular cross sections displayed in Figure 2 give us expectation that a large variety of new mo-

lecular assemblages can be designed. For instance, the distance between the surface polar groups may be controlled by using different sets of the tail. Two-dimensional distributions of particular functional groups may also be designed by taking advantage of limited component miscibility.

Acknowledgment. We extend our appreciation for financial support to Special Coordination Funds for Promoting Science and Technology from Science and Technology Agency of Japan.

Communications to the Editor

Chain Growth Rates in Fischer-Tropsch Synthesis on an Iron Catalyst: An Isotopic Transient Study

C. A. Mims* and L. E. McCandlish

*Exxon Research and Engineering Company
Corporate Research Laboratories
Annandale, New Jersey 08801*

Received October 9, 1984

We have examined the Fischer-Tropsch reaction by following both the rate and position of incorporation of ^{13}C into C_4 hydrocarbons after exchanging ^{13}CO for ^{12}CO in the reactant gas. Such isotopic transients under reaction steady state provide a valuable tool for the in situ study of catalytic reactions. The formation of CH_4 from CO and H_2 has been extensively studied by this technique,¹⁻⁴ and Biloen² has previously placed a lower bound on C-C bond formation rates by measuring the appearance rate of a new carbon isotope in C_3 fragments.

By examining both the rate and position of new label incorporation we are able to show that the major fraction of the hydrocarbon product at steady state derives from a much smaller number of growing chains than previously thought. Our data also place a lower limit to the average rate of chain growth in this system of two to four bonds per second.

The reaction was carried out in a small fixed bed reactor on 650 mg of promoted iron catalyst prepared in a manner similar to Dry's.⁵ Table I lists the experimental conditions which were chosen to maximize selectivity to terminal olefins. We determined the molecular distribution of the ingrowing label by GC/MS analysis⁶ of portions of the product gas sampled at selected times after the switch from ^{12}CO to ^{13}CO . NMR analysis of the intermediately labeled product revealed the location of the new label within the product molecules.

The evolution of the isotopic composition of the butene product is shown in Figure 1. A distribution of exchange rates for surface carbon is needed to describe the transient in Figure 1f, a fact consistent with previous reports by Biloen² and Bell.⁴ Determination of the total amount of "active" surface carbon is hampered by difficulty in integrating the long tail in the transient. Integration of the transient in Figure 1f to the point of 90% isotopic exchange shows that a small amount ($<1 \mu\text{mol}$ of C/g of catalyst)

Table I

| | |
|---|-----------|
| temp, K | 510 |
| H_2/CO ratio | 1.0 |
| total pressure, kPa | 90 |
| gas residence time, s | 0.15 |
| catalyst surface area (freshly reduced), $\text{m}^2 \text{g}^{-1}$ | ~ 40 |
| productivity, $\text{nmol s}^{-1} (\text{g of cat.})^{-1}$ | |
| C2 | 8.6 |
| C3 | 6.7 |
| C4 | 4.8 |
| C5 | 3.3 |
| C6 | 2.3 |
| olefin/paraffin | >10 |

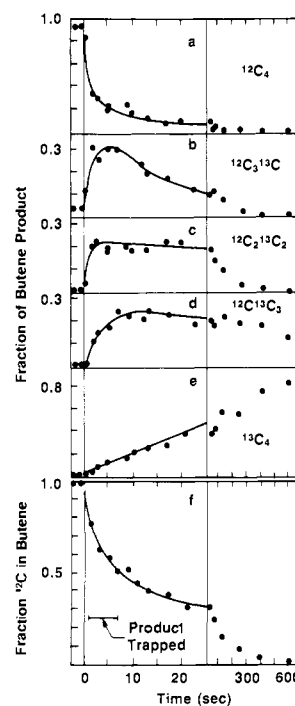


Figure 1. Evolution of ^{13}C into butene product after switch from ^{12}CO to ^{13}CO in reactant gas. (a-e) Distribution of the butene product among the isotopic variants $^{12}\text{C}_x^{13}\text{C}_{4-x}$. Note the change of time scale at 25 s. (f) The amount of ^{13}C in the butene product obtained by combination of data in (a-e). Product for NMR analysis was collected during the interval marked by the horizontal bar.

of surface carbon is responsible for 90% of the steady-state butene product. A more complete discussion of the transient kinetic behavior will be the subject of a separate paper.

The positional distribution of ^{13}C was determined by proton NMR analysis of transiently labeled product collected in the 6-s interval indicated in Figure 1.⁷ The collected product contains

(1) Happel, J.; Suzuki, I.; Kokayeff, P.; Fthenakis, V. *J. Catal.* **1980**, *65*, 59. Happel, J.; et al. *J. Catal.* **1982**, *75*, 314. Otarod, M.; et al. *J. Catal.* **1983**, *84*, 156.

(2) Biloen, P.; Helle, J. N.; van den Berg, F. G. A.; and Sachtler, W. M. H. *J. Catal.* **1983**, *81*, 450.

(3) Kobori, Y.; Yamasaki, H.; Naito, S.; Onishi, T.; Tamaru, K. *J. Chem. Soc., Faraday Trans. 1* **1982**, *78*, 1473.

(4) Cant, N. W.; Bell, A. T. *J. Catal.* **1982**, *73*, 257. Winslow, P.; Bell, A. T. *J. Catal.* **1984**, *86*, 158.

(5) Dry, M. E. "Catalysis: Science and Technology"; Anderson, J. R., Boudart, M., Eds.; Springer-Verlag: Berlin, 1981; Vol. 1, Chapter 4.

(6) GC/MS analysis rather than simple mass spectroscopy was necessary because of the extensive fragmentation of olefins even at rather low electron energies.

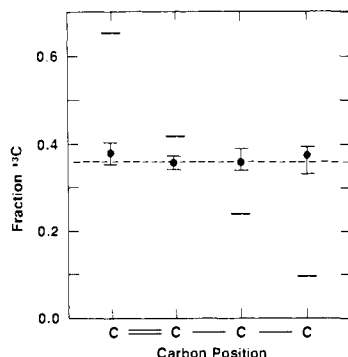


Figure 2. Fraction of ^{13}C at each position in the transiently labeled butene sample. The dashed horizontal line is the average value derived from GC/MS analysis. The short horizontal lines illustrate the anisotropy that would have resulted if only ^{13}C had been added sequentially to one end of the growing chains.

information about a major fraction of the steady-state hydrocarbon production since half the label had exchanged by the end of the collection interval. Results for 1-butene are shown here. The presence of ^{13}C at a given position in the molecule is revealed by the splitting of the proton resonance for that position. Any anisotropy seen in the positional distribution of the ^{13}C in the intermediately labeled molecules would indicate that the isotopic composition of the C_1 monomer changed appreciably fast compared to the rate of the chain propagation step. In this case, each successive carbon atom added to a given molecule after the isotope switch is significantly more likely to carry the ingrowing label. Such conditions would allow identification of the isotope exchange kinetics with chain growth kinetics. In addition, mechanisms in which carbon atoms are added to the end of the growing chain (e.g., alkyl migration⁸ or CO insertion⁹) could be distinguished from mechanisms with alternative growth steps.¹⁰

Figure 2 shows that within experimental error the label incorporation is isotropic. The butene chains collected here must have grown in a time much shorter than the time in which the isotopic composition of their surface precursors changed appreciably.¹¹ Modeling calculations show that the average butene molecule must have grown in less than 1 s. Under this condition, information about the mechanics of chain growth is lost. However, the rapid chain growth rate inferred from the isotropic ^{13}C incorporation means the amount of carbon in growing chains is much smaller than the amount of "active" carbon derived from our GC/MS data. From the butene production rate and the chain growth rate calculated here, we conclude that most of the butene product comes from fewer than 5 nmol of growing chains per g of catalyst. If we assume that the chain addition rate is independent of chain length, and if we use the Flory law to extrapolate the product distribution in Table I, we can estimate that at steady state fewer than 50 nmol of growing chains per g of catalyst are responsible for over half of all the C_2^+ hydrocarbon product. Modeling calculations and additional measurements will help refine this number and will take into account the fraction of product with longer isotope exchange times.

Acknowledgment. We thank K. D. Rose and R. E. Pabst, Jr., for NMR analyses and J. J. Krajewski for technical assistance.

Registry No. Iron, 7439-89-6; CO, 630-08-0.

(7) The accumulated product of 12 transients from 3 g of catalyst was separated by GC into its components and trapped in NMR tubes. This procedure yielded 250 nmol of butene which was examined in a JEOL 400-MHz NMR spectrometer.

(8) Biloen, P.; Helle, J. N.; Sachtler, W. M. H. *J. Catal.* **1979**, *58*, 95. Schulz, H. *Erdoel Kohle, Erdgas, Petrochem.* **1977**, *30*, 123.

(9) Wender, I.; Friedman, S.; Steinber, W. A.; Anderson, R. B. *Chem. Ind. (London)* **1958**, 1694.

(10) McCandlish, L. E. *J. Catal.* **1983**, *83*, 362.

(11) We have assumed that the chain integrity has not been compromised by scrambling. Our reaction conditions were chosen to limit the CO conversion to less than 1%. The fact that the reaction products are 1-olefins rather than the thermodynamically favored internal olefins suggests that secondary reactions which could scramble the position of the carbon atoms are absent.

Crystal Structure of the Neutral Diarylcuprate $\text{Cu}_2\text{Li}_2(\text{C}_6\text{H}_4\text{CH}_2\text{NMe}_2)_4$: The Asymmetric Bonding Configuration of Organo Groups Bridging Cu and Li

Gerard van Koten* and Johann T. B. H. Jastrzebski

Anorganisch Chemisch Laboratorium
University of Amsterdam, Nieuwe Achtergracht 166
1018 WV Amsterdam, The Netherlands

Fred Muller and Casper H. Stam

Laboratorium voor Krystallografie
University of Amsterdam, Nieuwe Achtergracht 166
1018 WV Amsterdam, The Netherlands

Received September 17, 1984

Reaction of an organolithium reagent, RLi , with a copper salt, Cu^1X , in a 2/1 molar ratio leads to the formation of a so-called lithium organocuprate reagent which has R_2CuLi overall stoichiometry. The unique change in reactivity brought about by this partial substitution of Li by Cu is of tremendous use in organic synthesis¹ and has also led to considerable interest in the bonding of the organo groups in these reagents.²

After many attempts³ we succeeded in growing single crystals of the cuprate⁴ $\text{Cu}_2\text{Li}_2(\text{C}_6\text{H}_4\text{CH}_2\text{NMe}_2)_4$ (**1**) which were suitable for an X-ray structure determination.⁵ The molecular structure of **1** is shown in Figure 1 together with some relevant bond distances and angles. To our knowledge this structure is the first example of a structural investigation of a neutral lithium organocuprate with 1/1 Cu/Li atomic ratio in the central metal core. Several other organocuprate structures have been reported which, however, all have ionic structures consisting of either mononuclear R_2Cu^- (Me_2Cu ,⁶ $[(\text{Me}_3\text{Si})_3\text{C}]_2\text{Cu}^-$) or polynuclear (i.e., $[\text{Cu}_3\text{Ph}_6]^-$)⁸ anions and solvated Li cations. Anionic $[\text{Cu}_3\text{Li}_2\text{Ph}_6]^-$ is the only other structurally characterized cuprate species known that contains both Li and Cu in the same metal framework.⁹

(1) For example: Posner, G. H. In "Organic Reactions, Substitution Reactions using Organocopper Reagents"; Wiley-Interscience: New York, 1982; Vol. 22, Chapter 2, p 253.

(2) (a) van Koten, G.; Jastrzebski, J. T. B. H.; Stam, C. H.; Brevard, C. "Copper Coordination Chemistry; Biochemical and Inorganic Perspectives"; Karlin, K. D., Zubieta, J., Eds.; Adenine Press: Guilderland, New York, 1985; in press. (b) van Koten, G.; Noltes, J. G. "Comprehensive Organometallic Chemistry"; Pergamon Press: New York, 1982; Vol. 14, p 709; *J. Am. Chem. Soc.* **1979**, *101*, 6593. Stewart, K. R.; Lever, J. R.; Whangbo, M.-H. *J. Org. Chem.* **1982**, *47*, 1472.

(3) In one crystallization from diethyl ether both yellow $\text{Cu}_4(\text{C}_6\text{H}_4\text{CH}_2\text{NMe}_2)_4$ and colorless crystals were formed. According to an X-ray structure determination the latter crystals appeared to be the lithium enolate ($\text{Li}_4(2\text{-H}_2\text{C}=\text{C}(\text{O})\text{C}_6\text{H}_4\text{CH}_2\text{NMe}_2)_4$, i.e., the product of an acetylation reaction at C(1): Jastrzebski, J. T. B. H.; van Koten, G., unpublished results.

(4) (a) The title compound was prepared by reacting pure $\text{Cu}_4(\text{C}_6\text{H}_4\text{CH}_2\text{NMe}_2)_4$ ^{2b} (5 mmol) with pure $\text{Li}_4(\text{C}_6\text{H}_4\text{CH}_2\text{NMe}_2)_4$ ^{4b} (5 mmol) in 10 mL of benzene. (b) Jastrzebski, J. T. B. H.; van Koten, G.; Konijn, M.; Stam, C. *J. Am. Chem. Soc.* **1982**, *104*, 5490.

(5) (a) Crystals of the title compound, $\text{Cu}_2\text{Li}_2\text{C}_{36}\text{H}_{38}\text{N}_4$, are monoclinic, space group $C2/c$, with four molecules in a unit cell of dimensions $a = 23.824$ (2) Å, $b = 9.614$ (2) Å, $c = 17.824$ (2) Å, and $\beta = 114.77(1)^\circ$. 3040 independent reflections measured on a NONIUS CAD 4 diffractometer using graphite monochromated Cu $K\alpha$ radiation. Of these 847 were below the $3\sigma(I)$ level and were treated as unobserved. An empirical absorption correction (DIF ABS)^{5b} was applied ($\mu = 15.8 \text{ cm}^{-1}$; crystal dimensions $0.23 \times 0.30 \times 0.50 \text{ mm}$). The structure was solved by means of a Patterson minimum function on the basis of the four translation-independent Cu positions in the unit cell and refined by means of block-diagonal least-square calculations, anisotropic for Cu, Li, C, and N and isotropic for H. The H atoms were located in a F synthesis. The final R value was 0.039 for 2193 reflections. An extinction correction was applied and a weighting scheme $w = 1/(5.2 + F_0 + 0.009F_0^2)$ was employed. The anomalous dispersion of Cu was taken into account. (b) Walker, N.; Stuart, D. *Acta Crystallogr., Sect. A* **1983**, *A39*, 158.

(6) Leoni, P.; Pasquali, M.; Ghilardi, C. A. *J. Chem. Soc., Chem. Commun.* **1983**, 241.

(7) Eaborn, C.; Hitchcock, P. B.; Smith, J. D.; Sullivan, A. C. *J. Organomet. Chem.* **1984**, *263*, C23.

(8) Edwards, P. G.; Gellert, R. W.; Marks, M. W.; Bau, R. *J. Am. Chem. Soc.* **1982**, *104*, 2072.